Cycloaddition Functionalizations to Preserve or Control the Conductance of Carbon Nanotubes

Young-Su Lee and Nicola Marzari
Department of Materials Science and Engineering, and Institute for Soldier Nanotechnologies, Massachusetts Institute of Technology, Cambridge, Massachusetts 02139, USA
(Dated: February 6, 2008)

We identify a class of covalent functionalizations that preserves or controls the conductance of single-walled metallic carbon nanotubes. [2+1] cycloadditions can induce bond cleaving between adjacent sidewall carbons, recovering in the process the sp^2 hybridization and the ideal conductance of the pristine tubes. This is radically at variance with the damage permanently induced by other common ligands, where a single covalent bond is formed with a sidewall carbon. Chirality, curvature, and chemistry determine bond cleaving, and in turn the electrical transport properties of a functionalized tube. A well-defined range of diameters can be found for which certain addends exhibit a bistable state, where the opening or closing of the sidewall bond, accompanied by a switch in the conductance, could be directed with chemical, optical or thermal means.

Chemical functionalizations of carbon nanotubes (CNTs) are the subject of intensive research [1, 2], and could offer new and promising avenues to process and assemble tubes, add sensing capabilities, or tune their electronic properties (e.g., doping levels, Schottky barriers, work functions, and electron-phonon couplings). However, the benefits of functionalizations are compromised by the damage to the conduction channels that follows sp^3 rehybridization of the sidewall carbons [3, 4], as evidenced by absorption spectra and electrical transport measurements [5, 6, 7]. We report here on a class of cycloaddition functionalizations that preserves instead the remarkable transport properties of metallic CNTs. In addition, we identify a subclass of addends that displays a reversible valence tautomerism that can directly control the conductance.

We focus here on [2+1] cycloaddition reactions, where the addition of a carbene or a nitrene group saturates a double-bond between two carbon atoms, forming a cyclopropane-like three-membered ring. Such functionalizations have been reported extensively in the literature [8, 9, 10]. All our calculations are performed using density-functional theory in the Perdew-Burke-Ernzerhof generalized gradient approximation (PBE-GGA) [11], ultrasoft pseudopotentials [12], a planewave basis set with a cutoff of 30 Ry for the wavefunctions and 240 Ry for the charge density, as implemented in Quantum-ESPRESSO [13].

We examine first the simplest members in this class of addends, CH_2 and NH. Fig. 1(a) and (b) show the two inequivalent choices available on a (5,5) metallic CNT; for convenience, we label these as "S" (skewed) and "O" (orthogonal), reminiscent of the relative positions of the sidewall carbons with respect to the tube axis. Our simulation cells include 12 n carbons for a given (n,n) CNT, plus one functional group. We use a 1×1×4 Monkhorst-Pack mesh (including Γ) for structural optimizations, and a 1×1×8 mesh for single-point energy calculations, with a cold smearing of 0.03 Ry [14].

First, and for (n,n) metallic tubes, we highlight how strongly the reaction energies of these functionalizations depend on the curvature of the nanotubes, and on their attachment sites S and O. We plot in Fig. 2(a) the reaction energies $\Delta E_{\rm CNT}$ (defined as $\Delta E_{\rm CNT} = E_{\rm CNT\text{-}func} - E_{\rm CNT} - E_{\rm func}$, func=$CH_2$ or NH), taking as a zero reference the same reaction on graphene. The reaction energies have a well-defined linear dependence on curvature, clearly demonstrating the higher reactivity of smaller-diameter tubes. The O site is always more stable, and significantly so for all diameters considered; at room temperature all small-diameter armchair CNTs strongly favor the O configuration. The energy difference between the O and the S form of the (5,5) CNT is 1.24 eV, which is in good agreement with other planewave basis calculations (1.24 eV, Ref. [15]) and localized basis calculations (1.4 eV, Ref. [16]).

Second, we find that the C_1-C_6 distance for this O configuration (d_{16} in Fig. 1(c)) is much larger than the usual C-C distance (1.54 Å in diamond and 1.42 Å in graphite), a clear indication that the sidewall bond is broken [15, 16, 17, 18]. For the CH_2 and NH cycloadditions, we observe bond cleaving for all nanotubes studied (up to (12,12)); on the other hand, in graphene the bond is intact. We estimate the critical diameter that sepa-

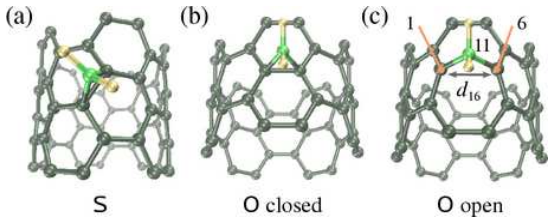

FIG. 1: The three different configurations for a functional group on an armchair nanotube are shown (CH_2 on a (5,5) CNT): (a) skewed S, (b) orthogonal O with an intact ("closed") sidewall bond, and (c) orthogonal O with a broken ("open") sidewall bond.

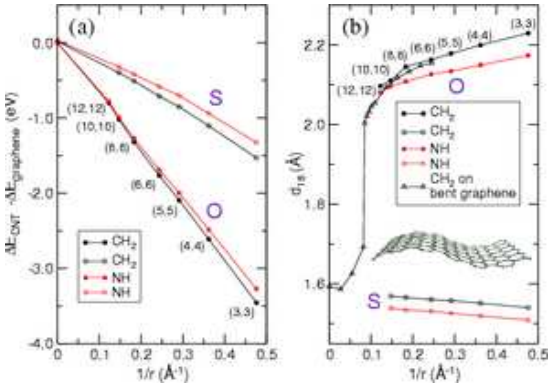

FIG. 2: (a) Energy change ΔE_{CNT} upon functionalization as a function of curvature, for (n,n) armchair CNTs - the zero reference is for graphene. (b) Sidewall equilibrium bond distance C_1-C_6 (d_{16}) for (n,n) CNTs and for a bent graphene sheet, functionalized at the stable O site. The sidewall bond is broken in all the (n,n) CNTs considered. Continuous bending of a graphene sheet shows that a well-defined transition from the closed to the open form takes place as the curvature increases.

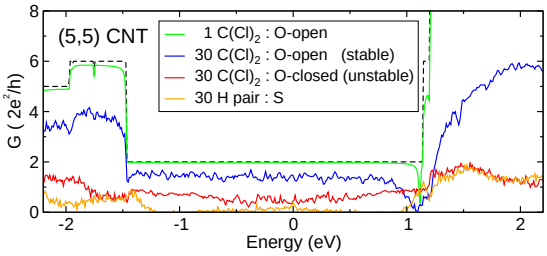

FIG. 3: Quantum conductance for a (5,5) CNT functionalized with one CCl_2 group, with 30 CCl_2 groups, and with 30 hydrogen pairs (dashed line: pristine (5,5) CNT). A CCl_2 addend will choose the O-open configuration, while hydrogens prefer to pair in the S configuration; the results corresponds to these stable choices. The conductance for the energetically-unstable O-closed configuration is also plotted. The 30 functional groups are arranged randomly on the central 43-nm segment of an otherwise infinite tube; the conductance is then averaged over 10 different configurations.

rates the two regimes by bending a graphene sheet: we can see in Fig. 2(b) that such model closely reproduces the nanotube results, and a sharp transition from the bond-intact to the bond-broken form takes place around a diameter of 2.4 nm, i.e. a (18,18) tube, for CH_2 functionalizations.

Broken or intact sidewall bonds play a fundamental role in the electronic transport properties of a metallic nanotube. We show this in Fig. 3, where the Landauer conductance is calculated for a (5,5) CNT functionalized with dichlorocarbene (CCl_2) (first reported experimentally in 1998 [8]), using an approach recently introduced by us that allows to treat realistic nanostructures with thousands of atoms while preserving full first-principles accuracy [4]. For this diameter the sidewall bond is broken, and the scattering by a single CCl_2 group is found to be remarkably weak, with the conductance approaching its ideal value. Even after adding 30 groups on the central 43 nm segment of an infinite nanotube the conductance is only reduced by 25%. This is in sharp contrast with the case of a hydrogenated tube, where the conductance drastically drops practically to zero when functionalized with a comparable number of ligands. This result is easily rationalized. Hydrogen and other single-bond covalent ligands induce sp^3 hybridization of the sidewall carbons, and these chemical defects act as very strong scatterers [4]. Such dramatic decrease in the conductance has also been recently confirmed experimentally [7]. On the other hand, after bond cleavage C_1 and C_6 recover a graphite-like bonding environment (Fig. 1(c)), with three covalent bonds to their nearest neighbors. Their electronic orbitals go back to sp^2 hybridization, allowing for the p_z orbitals of C_1 and C_6 to be recovered (as confirmed by inspection of the maximally-localized Wannier functions [19]) and to contribute again to the graphitic π manifold. The net result is that conductance approaches again that of a pristine CNT, highlighting the promise of cycloadditions in *preserving* the conductance of metallic nanotubes.

In principle, around the critical diameter shown in Fig. 2(b), a functional group could be found that displays as stable states on the same tube both the open and the closed configuration. If the case, interconversion between the two valence tautomers would have a direct effect on the conductance. We illustrate this paradigm with the dichlorocarbene example of Fig. 3; if we force the tube in its closed configuration, with all the sidewall bonds frozen in their ideal pristine-tube geometry, conductance decreases by a factor of 2 or 3 with respect to the case of the relaxed tube [20]. The configuration where the sidewall bonds are intact is not stable for this case, but, depending on the chemistry of the addends and the diameter considered, optimal ligands could be found for which a double-well stability is present.

In order to identify the factors that determine stability in the open or closed form, we first screen several addends on small molecules. We find that the bridged 1,6-X-[10]annulene (inset of Fig. 4(a)) is an excellent molecular homologue of a functionalized CNT [17]. It is well-known that the substitutional group X dictates the preference for the annulene (henceforth labelled as **1o**) or for its valence tautomer, a bisnorcaradiene derivative (**1c**), corresponding to the open and closed configurations of a functionalized CNT [22, 23, 24, 25, 26, 27]. Similar tautomerization between an open (**2o**) and a closed (**2c**) form takes place in a pyrene derivative [28] (inset of Fig. 4(b)). We thus tested on these molecules the substitutional groups X= CH_2, NH, SiH_2, $C(NO_2)_2$, $C(CN)_2$, $C(CCH)_2$, $C(CH_3)_2$, $C(COOH)_2$, CCl_2, $C(NH_2)_2$, C_6H_4O [29], and $C_{13}H_8$ [29]. To assess

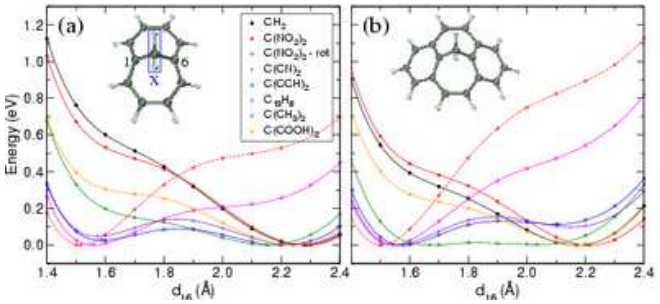

FIG. 4: Potential energy surface as a function of d_{16} for select cases of (a) **1** and (b) **2**. $C(CN)_2$ (violet) and $C(CCH)_2$ (blue) show a double-well minimum in both **1** and **2**. $C(NO_2)_2$-rot (dashed red) indicates the unstable conformation where the two NO_2 groups are rotated from their equilibrium position (solid red) by 90°.

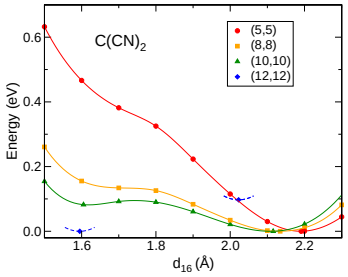

FIG. 5: Potential energy surface for (n,n) CNTs functionalized with $C(CN)_2$. Both (10,10) and (12,12) CNTs display a double-well minimum.

the accuracy of our PBE-GGA approach, we compare in Table I our results for d_{16} in **1** with those obtained from experiments or other theoretical methods (second order Møller-Plesset perturbation theory (MP2) [30] and Becke three parameter Lee-Yang-Parr hybrid functional (B3LYP) [31]), finding excellent agreement. Hydrogen and halogens have been reported to stabilize **1o** both experimentally and theoretically [24, 25, 32]. Cyano group favors **1c** experimentally (the possibility of coexistence with **1o** is discussed) [27], and two minima have been actually predicted theoretically [32, 35].

We show the potential energy profile of select groups in Fig. 4. All carbenes stabilizing the closed form in both **1** and **2** share a common feature: partially-occupied p orbitals parallel to the in-plane p_σ orbital of the bridgehead C_{11} atom [36] (the plane considered is that of C_1-C_{11}-C_6 of Fig. 1(c)). This conclusion is strongly supported by examining the energy minimum conformation for $X{=}C(NO_2)_2$. At equilibrium, the two oxygen atoms in the NO_2 group lie on a line parallel to the C_1-C_6 bond, and the open form is stable (solid red in Fig. 4). The sidewall bond will switch from open to closed upon rotation of the two NO_2 groups by 90° thereby placing the p orbitals of the nitrogens parallel to the p_σ orbital of C_{11} (dashed red in Fig. 4). Among all the substituents screened, we find that SiH_2, $C(CCH)_2$ and $C(CN)_2$ show most clearly the presence of two minima in their potential energy surface; we choose here $X{=}C(CN)_2$ as the most promising candidate since both **1c** [27] and a C_{60} derivative [37] have already been synthesized.

We explored, therefore, the potential energy landscape for armchair CNTs in the case of $C(CN)_2$ cycloadditions. The results shown in Fig. 5 reflect closely those found in the molecular homologues. A unique minimum in the open form is found in small-diameter tubes, as is generally the case in these [2+1] cycloadditions. As the diameter is increased, the signature of the closed minimum starts to appear, first as an inflection point ((5,5) CNT), then as a local minimum for the (10,10) CNT (ϕ=1.36 nm, as in **1c**), and finally as a global minimum for the (12,12) CNT (ϕ=1.63 nm, as in **2c**). As discussed before, the conductance is controlled by the bonding and hybridization of the sidewall carbons. We compare in Fig. 6 the two stable open and closed forms for the (10,10) CNT functionalized with $C(CN)_2$. The scattering induced by a single group is negligible, especially in the open form, and the conductance around the Fermi energy is extremely close to its ideal value (Fig. 6(a)). As the number of functional groups is increased, the difference between the two minima becomes rapidly apparent (Fig. 6(b)).

Two conclusions can be drawn: First, even with a large number of functional groups, the conductance of the tube is well preserved, whenever cycloaddition breaks the sidewall bond. Second, a subclass of substituents can be found (e.g., $C(CN)_2$) that stabilize two tautomeric forms on the same tube, separately displaying high and low conductance. Several mechanisms, including photochemical, electrochemical, and thermal, could then direct interconversion between the two tautomeric forms. Photochemical and electrochemical interconversion rely on the fact that the energy levels of the frontier orbitals are affected by d_{16}, depending on their symmetries and charge distri-

TABLE I: Experimental and theoretical d_{16} of **1**. Note that the calculations assume isolated molecules at 0 K, while experimental data are obtained from crystalline systems at finite temperature. Theory predicts two stable minima for $X{=}C(CN)_2$. The long d_{16} of $X{=}C(CH_3)_2$ indicates that the potential energy surface would be very flat, which is also predicted in Fig. 4, especially for **2**.

X	Expt.	MP2	B3LYP	This work
CH_2	2.235[a]	2.251[f]	2.279[g]	2.278
CF_2	2.269[b]	2.268[f]	2.296[f]	2.300
$C(CN)_2$	1.542[c]	1.599, 2.237[f]	1.558, 2.253[h]	1.572, 2.245
$C(CH_3)_2$	1.836[d]	2.156[f]	2.168[f]	2.151
NH	(open)[e]		2.237[g]	2.239

[a]Ref. [25], [b]Ref. [24], [c]Ref. [27], [d]Ref. [22], [e]Ref. [33], [f]Ref. [32], [g]Ref. [34], [h]Ref. [35]

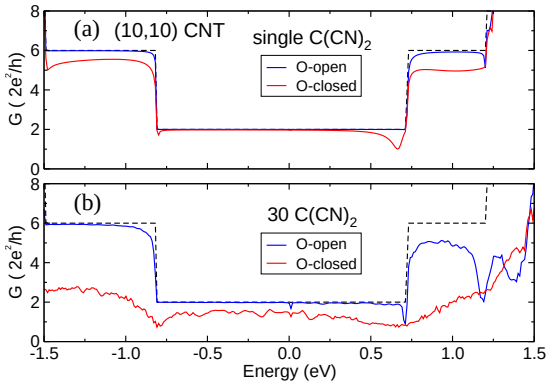

FIG. 6: Quantum conductance for a (10,10) CNT functionalized with $C(CN)_2$, in the O-open and O-closed stable configurations (dashed line: pristine (10,10) CNT). (a) Single group. (b) 30 functional groups arranged randomly on the central 32-nm segment of an infinite tube; the conductance is then averaged over 10 different configurations.

butions (e.g., the bond weakens as a filled orbital that has bonding character along C_1-C_6 is emptied) [32, 36]. Both photochemical excitations or electrochemical reduction or oxidation can populate or depopulate those frontier orbitals that favor the open or closed form; as a result, they would modulate the bond distance, and ultimately the conductance. As a proof of principle, time-dependent density functional calculations in **2** for $X{=}C(CN)_2$ show that the first singlet excitation (S_1) drives the system from the open to the closed form [38]. A similar conclusion is drawn from experimental observations in **2o** for $X{=}CH_2$, where this open form is stable in the ground state while the closed **2c** is presumed to be stable in the S_1 energy surface [28]. Temperature also plays an important role, and ^{13}C NMR spectroscopy and X-ray data have captured the temperature-dependent equilibrium of similar fluxional systems: a higher temperature stabilizes **1o** for $X{=}C(CN)(CH_3)$, while destabilizing it for $X{=}C(CH_3)_2$ [23, 26].

In conclusion, our calculations predict that 1) a broad class of cycloaddition functionalizations on narrow-diameter nanotubes recovers, as a consequence of bond cleaving, the conductance of the original pristine tubes, allowing for organic chemistry approaches to manipulation and assembly that preserve the remarkable electronic properties of these materials, and 2) that a subclass of addends, exemplified in this work by dicyanocarbene, exhibits fluxional behavior that could be controlled with optical or electrochemical means. Such conductance control, if realized, could have practical applications in nano- and opto-electronics, chemical sensing, and imaging.

The authors would like to thank Francesco Stellacci (MIT) and Maurizio Prato (University of Trieste) for helpful discussions. This research has been supported by MIT Institute for Soldier Nanotechnologies (ISN-ARO DAAD 19-02-D-0002) and the National Science Foundation (DMR-0304019); computational facilities have been provided through NSF (DMR-0414849) and PNNL (EMSL-UP-9597).

[1] C. A. Dyke and J. M. Tour, J. Phys. Chem. A **108**, 11151 (2004).
[2] X. Lu and Z. Chen, Chem. Rev. **105**, 3643 (2005).
[3] K. Kamaras *et al.*, Science **301**, 1501 (2003).
[4] Y.-S. Lee, M. B. Nardelli, and N. Marzari, Phys. Rev. Lett. **95**, 076804 (2005).
[5] M. S. Strano *et al.*, Science **301**, 1519 (2003).
[6] C. Wang *et al.*, J. Am. Chem. Soc. **127**, 11460 (2005).
[7] C. Klinke *et al.*, Nano Lett. **6**, 906 (2006).
[8] J. Chen *et al.*, Science **282**, 95 (1998).
[9] M. Holzinger *et al.*, Angew. Chem. Int. Ed. **40**, 4002 (2001).
[10] K. S. Coleman, S. R. Bailey, S. Fogden, and M. L. H. Green, J. Am. Chem. Soc. **125**, 8722 (2003).
[11] J. P. Perdew, K. Burke, and M. Ernzerhof, Phys. Rev. Lett. **77**, 3865 (1996).
[12] D. Vanderbilt, Phys. Rev. B **41**, 7892 (1990).
[13] S. Baroni *et al.*, http://www.quantum-espresso.org.
[14] N. Marzari *et al.*, Phys. Rev. Lett. **82**, 3296 (1999).
[15] J. Lu *et al.*, J. Mol. Struct. (Theochem) **725**, 255 (2005).
[16] H. F. Bettinger, Chem. Eur. J. **12**, 4372 (2006).
[17] Z. Chen *et al.*, Angew. Chem. Int. Ed. **43**, 1552 (2004).
[18] J. Zhao *et al.*, ChemPhysChem **6**, 598 (2005).
[19] N. Marzari and D. Vanderbilt, Phys. Rev. B **56**, 12847 (1997).
[20] A recent study that considered a (6,6) CNT functionalized with CCl_2 did not find that the open configuration displays higher conductance [21]; we ascribe this discrepancy to the lack of chemical accuracy in the model Hückel Hamiltonian used.
[21] H. Park, J. Zhao, and J. P. Lu, Nano Lett. **6**, 916 (2006).
[22] R. Bianchi *et al.*, Acta Crystallogr. **B29**, 1196 (1973).
[23] H. Günther and H. Schmickler, Pure Appl. Chem. **44**, 807 (1975).
[24] T. Pilati and M. Simonetta, Acta Crystallogr. **B32**, 1912 (1976).
[25] R. Bianchi, T. Pilati, and M. Simonetta, Acta Crystallogr. **B36**, 3146 (1980).
[26] R. Bianchi, T. Pilati, and M. Simonetta, J. Am. Chem. Soc. **103**, 6426 (1981).
[27] E. Vogel *et al.*, Angew. Chem. Int. Ed. Engl. **21**, 869 (1982).
[28] J. Wirz *et al.*, Helv. Chim. Acta **67**, 305 (1984).
[29] M. Eiermann *et al.*, Angew. Chem. Int. Ed. Engl. **34**, 1591 (1995).
[30] C. Møller and M. S. Plesset, Phys. Rev. **46**, 618 (1934).
[31] A. D. Becke, J. Chem. Phys. **98**, 1372 (1993); C. Lee, W. Yang, and R. G. Parr, Phys. Rev. B **37**, 785 (1988).
[32] C. H. Choi and M. Kertesz, J. Phys. Chem. A **102**, 3429 (1998).
[33] E. Vogel, W. Pretzer, and W. A. Böll, Tetrahedron Lett. **6**, 3613 (1965).
[34] H. J. Jiao, N. J. R. v. E. Hommes, and P. v. R. Schleyer, Org. Lett. **4**, 2393 (2002).
[35] C. Gellini, P. R. Salvi, and E. Vogel, J. Phys. Chem. A **104**, 3110 (2000).

[36] C. Mealli *et al.*, Chem. Eur. J. **3**, 958 (1997).
[37] M. Keshavarz-K *et al.*, Tetrahedron **52**, 5149 (1996).
[38] Y.-S. Lee *et al.*, in preparation.